2025 IEEE 21st International Conference on Automation Science and Engineering (CASE)
August 17-21, 2025. Los Angeles, CA, US

2025 IEEE 21st International Conference on Automation Science and Engineering (CASE) | 979-8-3315-2246-9/25/$31.00 ©2025 IEEE | DOI: 10.1109/CASE58245.2025.11163893

Novel Gaits for Snake Robot Navigation in Complex External Pipe Networks

Karthik Karumanchi[1], Sylvain Pellegrini[2], Andrew Orekhov[2], Yizhu Gu[2], Ralph Boirum[2], Bhaskar Vundurthy[2], and Howie Choset[2]

***Abstract*— This paper introduces novel locomotion strategies for snake robots navigating complex external pipe networks, addressing challenges beyond simple pipe traversal. Existing gait-based control methods struggle with obstacles like valves and complex junctions such as T-shaped intersections. To overcome these limitations, we propose two new gaits: the spiraling gait and the windowed rolling helix gait. The spiraling gait enables autonomous obstacle avoidance by rotating the robot in a helical motion around the pipe axis, effectively navigating around obstructions. The windowed rolling helix gait facilitates seamless traversal of T-shaped junctions by allowing the robot to selectively extend and shift segments, enabling transitions between pipe branches with minimal user intervention. Experimental results demonstrate the effectiveness of these gaits in navigating diverse external pipe features, showcasing improved adaptability and autonomy compared to existing methods. This work advances snake robot capabilities for robust inspection and maintenance in complex industrial environments.**

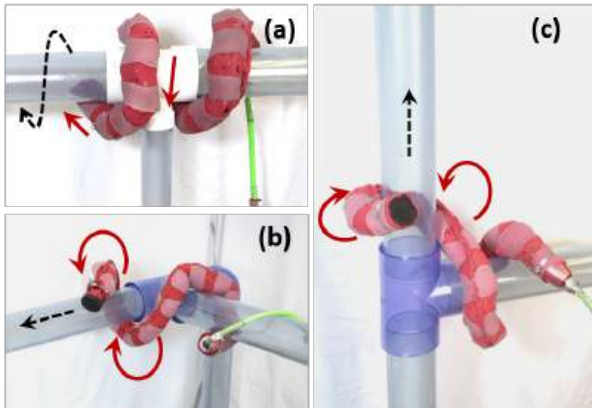

Fig. 1: Snake robot navigation. (a) *Spiraling gait* around an obstruction. (b) Horizontal and (c) vertical T-shaped junction traversal using *windowed rolling helix gait*. Red arrows: module motion; black dashed arrows: robot's travel direction.

I. Introduction

Complex pipe networks, characterized by intricate junctions, elbows, and varying structural elements, are critical in industries like chemical processing, power generation, and residential water distribution. These complexities, coupled with inherent inaccessibility and safety concerns, necessitate the deployment of robust robotic systems for reliable pipe network inspection. Traditional wheeled [1]–[3] or tracked [4], [5] robots often struggle with these complex environments due to their rigid designs. In contrast, snake robots [6], by virtue of their many degrees of freedom, adapt their shapes to navigate these intricate structures (see Fig. 1), offering a versatile and effective approach to comprehensive pipe network inspection.

Pipe network navigation encompasses two distinct domains: confined internal traversal focusing on in-situ inspection and maintenance within the pipe's bore, and unconfined external locomotion enabling manipulation and navigation along the complex external contours to address structural integrity and accessibility challenges. The inherent flexibility of snake robots, achieved through numerous serially connected actuated links, enables them to adapt to these diverse navigation scenarios. However, this flexibility introduces the challenge of coordinating an increasing number of joints. To address this, prior research has extensively utilized parametrized cyclic gaits [7]–[10]. These gaits effectively reduce the complex task of joint coordination to the manipulation of a limited set of parameters, facilitating robust and repeatable motion in both internal and external pipe environments.

Studies on gait-based control for pipe navigation have explored both internal and external domains. In internal navigation, research has explored in-pipe traversal, encompassing locomotion through complex pipe networks with varying diameters and junctions [11], [12], and modified helical rolling motion for large bending radius turns [13]. In contrast, external pipe navigation, while showing promise in climbing straight pipes [14], [15], faces additional complexities. Real-world pipe networks rarely consist of straight sections alone and are interspersed with junctions, bends, and obstacles such as valves and clamps. This introduces challenges not encountered in internal pipe traversal, as the robot is no longer constrained and guided by the pipe's geometry. While large bending radius turns can be traversed with minor modifications to existing pipe traversal gaits [13], prior works have not demonstrated navigation of more complex external features such as T-shaped junctions and obstacles.

To address the limitations of existing gait-based control of external pipe navigation, this paper introduces two novel locomotion strategies: the *spiraling gait* and the *windowed rolling helix gait*. The spiraling gait builds upon the rolling helix gait proposed by Hatton et. al. [14]. It enables the snake robot to navigate around external obstacles by rotating around the pipe axis in a screw-like helical motion (see Fig.

[1] Karthik Karumanchi is from the Department of Mechanical Engineering, Carnegie Mellon University, USA. kkaruman@andrew.cmu.edu
[2] The authors are affiliated with The Robotics Institute, Carnegie Mellon University, USA. {sylvainp, aorekhov7, yizhug, rboirum, pvundurt, choset}@andrew.cmu.edu

1(a)). Examples of these obstacles include valves and clamps. Once activated by the user, this gait operates autonomously and adds an obstacle avoidance capability to the existing rolling helix gait.

Similarly, the windowed rolling helix gait also builds upon the rolling helix gait and is designed for traversing T-shaped junctions (see Fig. 1(b) and 1(c)), enabling seamless transition between pipe segments. This novel gait requires the human operator to specify the direction of movement beyond the T-shaped junction, effectively indicating whether to turn left or right. Then, a portion of the snake robot reaches out to the new pipe segment. Subsequently, the remaining modules are shifted from the current segment to the new one. This automated process facilitates navigation through complex pipe networks with minimal human intervention.

The remainder of the paper is structured as follows. Section II reviews prior work on snake robot pipe network navigation. Section III outlines the framework for gait-based control from prior works and details the rolling helix gait. Sections IV and V describe the algorithms developed for executing the spiraling and windowed rolling helix gaits. Section VI presents experimental results demonstrating navigation across various junctions and obstacles. Finally, Section VII discusses conclusions and future work.

II. Prior Work

Gait-based control of snake robots often relies on inferring joint angles from a "backbone curve", a concept pioneered by Chirikjian and Burdick [16]. These joint angles can be determined directly using the serpenoid equation [17] or through the numerical integration of shape functions [18]. A notable gait, the *rolling helix*, introduced by Hatton and Choset [14], enables snake robots to navigate straight sections of pipes, both internally and externally.

Several researchers have extended the rolling helix gait to handle more complex scenarios. Nakajima et al. [19] and Qi et al. [20] proposed modifications involving manually controlled "rolling" and "shifting" waves to navigate branch points. Similarly, Kamegawa et al. [13] addressed large radius bends within pipes by designing bent helical curves using shape functions, requiring a human operator to switch between regular and bent helical behaviors.

Furthermore, Rollinson et al. [11] and Inazawa et al. [12] tackled T-shaped junctions inside pipes. Rollinson et. al. [11] utilized an Extended Kalman Filter to estimate the snake robot's state and propagate a bend along its length, while Inazawa et. al. [12] developed parametric curves for different junction geometries, which were numerically integrated. Both of these methods required consistent user input during navigation.

This work focuses on exterior pipe network navigation, specifically addressing T-shaped junctions and obstructions, with the goal of minimizing user intervention. Unlike the approaches relying on numerical integration of shape functions, this study employs the serpenoid equation for joint angle generation, eliminating the need for iterative computations at each time step.

III. Rolling Helix Gait

In this section, we present the mathematical framework for gait-based control in snake robots. We also present details about an existing gait: the rolling helix [14]. Subsequent sections augment the rolling helix gait to navigate complex features of a pipe network.

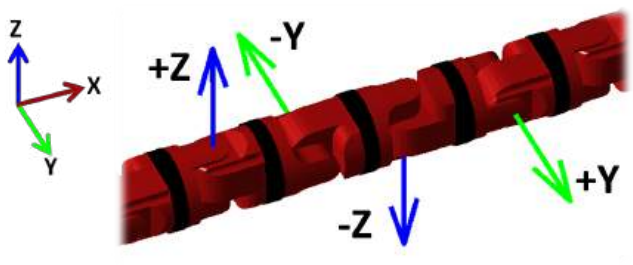

Fig. 2: Kinematic configuration of the snake robot. Blue lines indicate axes of rotation for dorsal joints and green lines indicate axes of rotation for lateral joints. Each joint's axis of rotation is offset from the previous joint by 90^0.

Our snake robots are comprised of 16 single degree of freedom (1-DOF) joints alternately oriented in the lateral and dorsal planes, as shown in Fig. 2. To coordinate these degrees of freedom, we employ the serpenoid equation [17] and its 3D extension [21]. The general form of the compound serpenoid equation commands lateral and dorsal joint angles.

$$\begin{aligned} \alpha_{lat}(n,t) &= \beta_{lat} + A_{lat}\sin(\theta_{lat}(n,t)) \\ \alpha_{dor}(n,t) &= \beta_{dor} + A_{dor}\sin(\theta_{dor}(n,t) + \delta) \end{aligned} \tag{1}$$

$$\begin{aligned} \theta_{lat}(n,t) &= \omega_{s,lat} n + \omega_{t,lat} t \\ \theta_{dor}(n,t) &= \omega_{s,dor} n + \omega_{t,dor} t \end{aligned} \tag{2}$$

In (1), α_{lat} and α_{dor} represent the lateral and dorsal joint angles and are parameterized by the angular offset β, amplitude A and phase offset δ. In (2), ω_s describes the spatial frequency of waves with respect to the module number $n \in \{0, \ldots, N-1\}$, where N is the total number of modules. ω_t, on the other hand, describes the temporal frequency of the actuators with respect to time t.

The rolling helix gait $\mathcal{H}$, a snapshot of which is shown in Fig. 3, is derived by commanding the same lateral and dorsal waves offset by $\pi/2$ to form a helix of constant curvature:

$$\mathcal{H}(n,t): \begin{cases} \alpha_{lat}(n,t) = A\sin(\omega_s n + \omega_t t) \\ \alpha_{dor}(n,t) = A\sin(\omega_s n + \omega_t t + \pi/2) \end{cases} \tag{3}$$

Fig. 3: A snapshot of the snake robot executing the rolling helix gait to traverse straight pipes oriented horizontally. It is described by lateral and dorsal waves which are equal in magnitude but offset by $\delta = \pi/2$.

Amplitude A, the spatial frequency ω_s, and the module length l_M uniquely determine the radius r, pitch p and handedness ν of the helix [22]:

$$\begin{aligned} p &= \frac{l_M}{\left(\left(\frac{A}{2\sin(\omega_s)}\right)^2 + 1\right)\omega_s} \\ r &= \frac{A}{2\sin(\omega_s)} p \\ \nu &= \text{sgn}(A\omega_s) \end{aligned} \tag{4}$$

Initial values for the gait parameters to climb a given pipe can be calculated from (4), which are then tuned to ensure the robot grips the pipe with enough friction for forward motion. In practice, a value for the amplitude higher than that obtained from (4) ensures adequate grip.

IV. Spiraling Gait

In this section, we present a spiraling gait (Algorithm 1) that allows the robot to rotate around the central axis of a pipe in a screw-like motion. This gait can be used to avoid obstacles such as valves or clamps, as shown in Section VI. During the spiraling gait, a "pulse" (blue region in Fig. 4) is propagated from the tail (n = 0) to the head ($n = N-1$).

Modules within the pulse's width form a helix with a larger radius, while the remaining modules maintain the helix described by the original gait equations. The pulse's width around $n = n_s$ is defined by an activation function s. Joint angles α are given by:

$$\begin{aligned} \alpha_s(n,t) =& \mathcal{H}(n,t|A^p,\omega_s^p)s(n,n_s) + \\ & \mathcal{H}(n,t|A,\omega_s)(1-s(n,n_s)) \end{aligned} \tag{5}$$

where, $\mathcal{H}(n,t|A,\omega_s)$ is the rolling helix gait parameterized by amplitude A and spatial frequency ω_s. The pulse is centered at $n = n_s$ and is parameterized by amplitude A_p and spatial frequency ω_s^p:

$$\omega_s^p = \frac{(k_p p) l_M}{(k_r r)^2 + (k_p p)^2}$$

$$A^p = 2\frac{(k_r r)}{(k_p p)} sin(\omega_s^p) \tag{6}$$

where, p and r are the pitch and radius of the original helix, while $k_p p$ and $k_r r$ are the pitch and radius of the helix described by the pulse.

Lastly, the activation function s is described by exponential functions as follows:

$$s(n,n_s) = \frac{1}{1+e^{-m(n-(n_s-0.5))}} + \frac{1}{1+e^{-m((n_s+0.5)-n)}} - 1 \tag{7}$$

where, m controls the slope of the exponential function around the pulse location $n = n_s$.

Algorithm 1: Spiraling Algorithm

Inputs : Rolling Helix gait $\mathcal{H}(n,t|A,\omega_s)$,
Total gait execution time ΔT_s
Gait activation time T_0
Data : Number of modules N,
Loop rate Δt,
Pulse velocity $\frac{dn_s}{dt}$
Outputs : Joint angles α at each time t

```
Initialize: n_s := N − 1
while t < T_0 + ΔT_s do
    for n = 0 to N-1 do
        Compute joint angles α(n,t) using (6)
        if n_s < 0 then
            Reset pulse location to N − 1
        else
            Update the pulse location by (dn_s/dt) Δt
        end
        Increment time t by Δt
    end
end
```

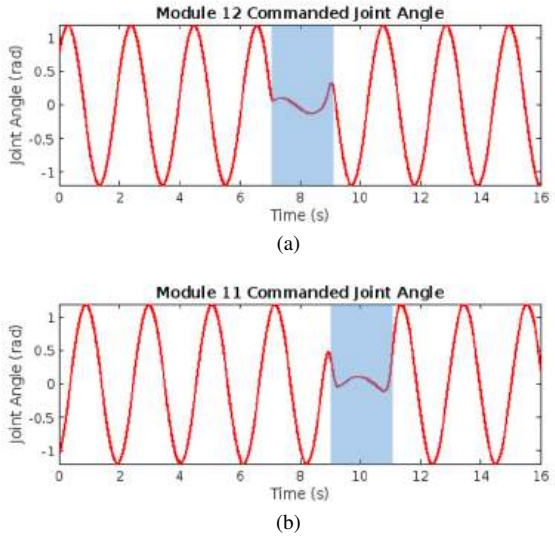

(a)

(b)

Fig. 4: Spiraling gait joint angles with respect to time for (a) module 12 and (b) module 11. When the pulse passes through a module, the helix radius increases, resulting in a low amplitude wave (highlighted in blue). Once the pulse passes, the original rolling helix gait is resumed.

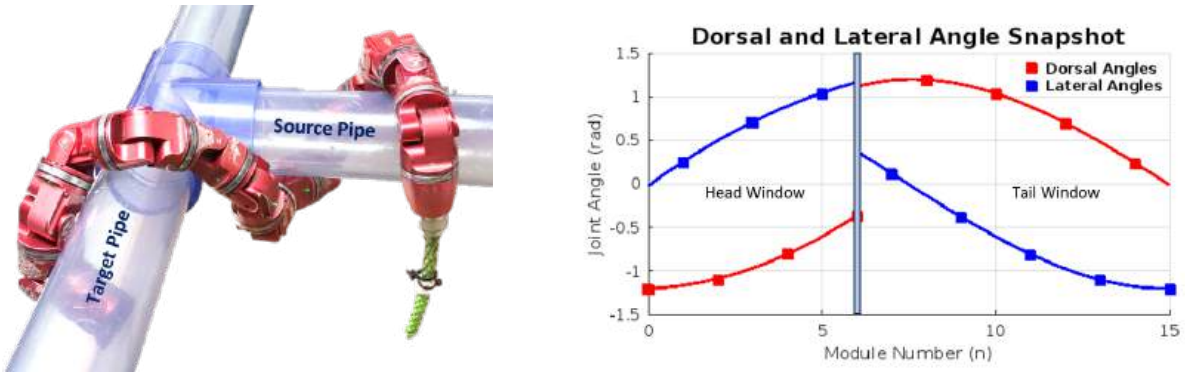

(a) (b)

Fig. 5: (a) A configuration of the robot executing the windowed rolling helix gait and (b) the corresponding dorsal and lateral joint angles for the head and tail windows. The first 7 modules of the snake belong to the head window and the remaining to the tail window. Gaits in the two windows are offset by $\pi/2$, leading to the discontinuity at $n = 6$.

V. Windowed Rolling Helix Gait

In this section, we develop a modification on the rolling helix gait presented in Section III that defines two helices on "windows" with perpendicular centerline axes. We utilize this modification to develop an algorithm to navigate over T-shaped junctions.

A. Modification to the Rolling Helix Gait

To navigate junctions, the rolling helix gait was extended by splitting the snake into head and tail "windows". The tail window governs the portion of the snake robot on the source pipe while the head window controls the portion on the target pipe as depicted in Fig. 5. Each window operates its own rolling helix gait described in (8)

$$\mathcal{H}^{head}(n,t): \begin{cases} \alpha^h_{lat}(n,t) = A sin(\omega_s n + \omega_t t) \\ \alpha^h_{dor}(n,t) = A sin(\omega_s n + \omega_t t + \pi/2) \end{cases}$$

$$\mathcal{H}^{tail}(n,t): \begin{cases} \alpha^t_{lat}(n,t) = A sin(\omega_s n + \omega_t t + \Delta_w) \\ \alpha^t_{dor}(n,t) = A sin(\omega_s n + \omega_t t + \pi/2 + \Delta_w) \end{cases} \tag{8}$$

where $\delta(= \pi/2)$ represents the phase offset between lateral and dorsal joints within a window and Δ_w represents an offset between gaits of the head and tail windows.

To navigate T-shaped junctions where pipes are perpendicular to each other, this gait offset is set as follows:

$$\Delta_w = -\nu \frac{\pi}{2} \tag{9}$$

B. T-shaped Junction Navigation Algorithm

In this section, we first present four key aspects of navigating a T-junction with a snake robot. Algorithm 2 then utilizes these aspects along with the windowed rolling helix gait from Section V-A to navigate the T-junction.

Algorithm 2: T-shaped junction Navigation Algorithm

Inputs : Rolling Helix gait $\mathcal{H}(n,t|A,\omega_s)$
User-indicated module n_b^u
Data : Number of modules N,
Loop rate Δt
Outputs : Joint angles α at each time t

Initialize: Transition location $n_t := 0$
Estimate Pipe Diameter as per (13)
Estimate number of bend modules n_b using (11)
if $|n_b - n_b^u|$ **then**
  Execute Spiraling gait for $\frac{\Delta T_s}{(n_b - n_b^u)}$ seconds
end
Define gaits for head and tail windows using (8)
while $n_t \leq N$ **do**
  for *n = 0* **to** *N-1* **do**
    if $n \leq n_t$ **then**
      Compute $\alpha(n,t)$ using $\mathcal{H}^{head}$
    else
      Compute $\alpha(n,t)$ using $\mathcal{H}^{tail}$
    end
  end
  Apply loosening function $\mathcal{L}$ (12) to bend modules
  Update the transition location using (10)
end

1) Window Propagation: From Section V-A, modules of the snake on each pipe are controlled by distinct windows. As navigation progresses, more modules shift from the source pipe onto the target pipe. This shift between the two windows is tracked by the transition location, denoted n_t.

From (3), for each actuator cycle lasting $1/\omega_t$ seconds, the snake robot moves forward on a pipe by πd_M where d_M is the diameter of a module. By the time the snake robot moves one module length forward, the transition location n_t must move one module tail-ward. Thus, the transition location is

updated as:

$$\dot{n_t} = \frac{l_M}{\pi d_M \omega_t} \tag{10}$$

2) Bend Modules: To begin transferring modules from the source to the target pipe, modules at the snake's head ($n \in [0, ..., n_b - 1]$) must let go of the source pipe and reach out to the target pipe. These n_b modules are termed "bend modules". Through empirical observations, we have found that a good choice for the number of bend modules n_b (11) corresponds to the modules wrapping approximately three-quarters of a full turn around the target pipe (with a diameter d_{pipe}).

$$n_b = \left\lfloor \frac{3\pi}{4} \frac{d_{pipe} + d_M}{l_M} \right\rfloor \tag{11}$$

3) Loosening Function: From Section III, rolling helix gaits squeeze the pipes in order to generate sufficient grip for movement. This tightness poses a problem for bend modules as they reach out to the target pipe. Without an opposing force, these modules curl onto themselves and fail to wrap around the target pipe. To prevent this, the loosening function (12) $\mathcal{L}$ reduces their amplitude, as shown in Fig. 6, until all bend modules have transferred to the target pipe, which occurs at $n_t = n_b$.

$$\mathcal{H}^{head}(n,t)\Big|_{n\in[0,n_b-1]} = \mathcal{L}(n_t|n_b)\mathcal{H}^{head}(n,t)$$
$$\mathcal{L}(n_t|n_b) = k_{low} + \frac{1-k_{low}}{1+e^{-m(n_t-n_b)}} \tag{12}$$

where, k_{low} and m represent the unwrapped amplitude and the sharpness of the amplitude increase around $n = n_b$ respectively.

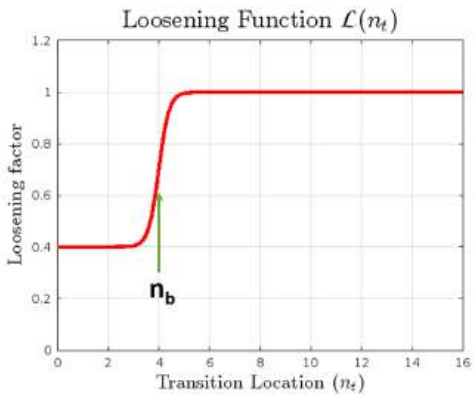

Fig. 6: Loosening function $\mathcal{L}(n_t)$ against transition location n_t for 4 bend modules. k_{low} controls the initial unwrapped amplitude and m controls the slope of the curve around $n_t = n_b$. $k_{low} = 0.4$ and $m = 5$ were found to work well in tests. The head window amplitude is multiplied by this factor and applied to the bend modules as they wrap onto the target pipe.

4) State Estimation using Virtual Chassis: From V-B.2, the number of bend modules depends on the diameter of the target pipe. To estimate the diameter, we first construct a virtual chassis proposed by Rollinson et al. [23]. The virtual chassis helps identify the principal component directions in the snake's body frame, as shown in Fig. 7. For a helical shape, two principal directions lie along the radial directions, while the third direction lies along the helix axis. The diameter is then estimated from the average radius along the radial principal directions:

$$\hat{d}_{pipe} = \frac{2}{N}\left(\sum_{n=0}^{N} ||(r_n^b \cdot p^{r_1})p^{r_1} + (r_n^b \cdot p^{r_2})p^{r_2}||_2\right) - d_M \tag{13}$$

In (13), r_n^b is the position of module n in a frame whose axes are aligned with the principal directions. $p^{r_{1,2}}$ are the radial principal directions and $\hat{d}_{pipe}$ is the estimated pipe diameter.

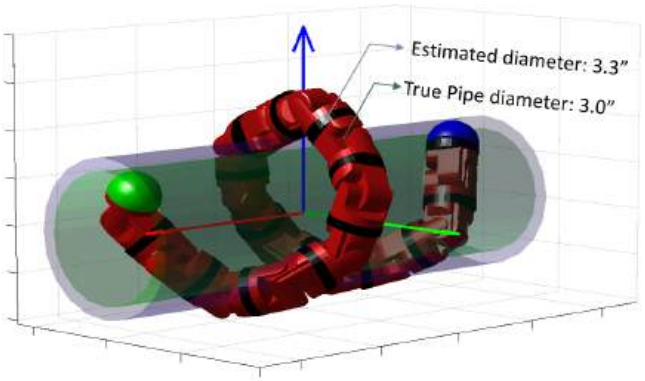

Fig. 7: Pipe diameter estimation using virtual chassis. Principal directions obtained from virtual chassis are marked in the figure. The average norm of module positions along the radial principal directions are used to estimate the pipe diameter. Section VI shows that this approach can estimate the pipe diameter to within 10% of the true diameter.

VI. Experimental Results

Experiments were run to test the spiraling and windowed rolling helix gaits on a pipe network (Fig. 11) comprised of 3 in pipes with an outer diameter of 88.90 mm (3.5 in). The network featured junctions at various orientations and obstructions demonstrating the snake robot's ability to overcome gravity during navigation. Videos of these experiments can be accessed at [*https://sites.google.com/andrew.cmu.edu/snake-pipe-network/home*].

The Series-Elastic Actuated (SEA) snake robot [24] was used in these experiments. Each joint has a range of motion of $\pm 90^0$ and is capable of delivering a torque up to 4 Nm. Modules of the SEA snake have a diameter of 50.80 mm (2 in) and a joint-to-joint distance of 66.04 mm (2.6 in). The SEA snake is also covered by a skin to provide additional grip with the pipes. This skin is made of nylon with intermittent silicone strips. Silicone enhances grip while nylon allows the joints to actuate freely.

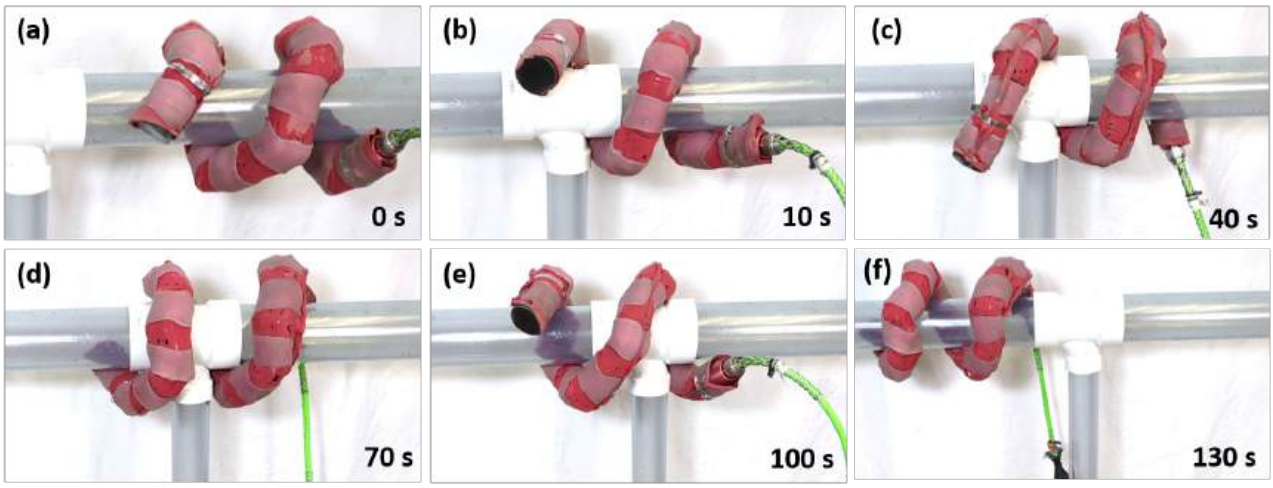

Fig. 8: Stills from a video of the snake robot executing a spiraling gait while navigating around a sink pipe. The sink pipe is treated as an obstacle for pipe navigation. The user triggers the spiraling gait when sufficiently close to the sink pipe. However, the execution of screw-like behavior, characteristic to the spiraling gait is performed autonomously.

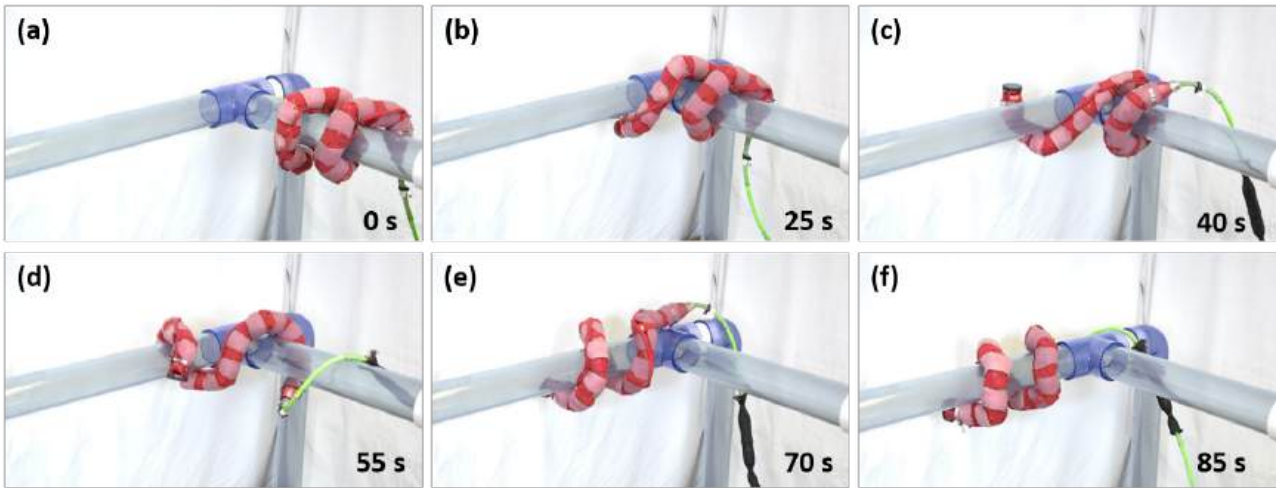

Fig. 9: Stills from videos of the snake robot navigating a T-shaped junction in the horizontal plane. Each test involves (a) navigating to the T-shaped junction, (b) bend modules letting go of the source pipe, (c) bend modules wrapping onto the target pipe, (d,e) modules transferring from the source to the target pipe and lastly, (f) navigating away from the T-shaped junction on the target pipe. Of these, all except the first (a) and last (f) steps are performed autonomously.

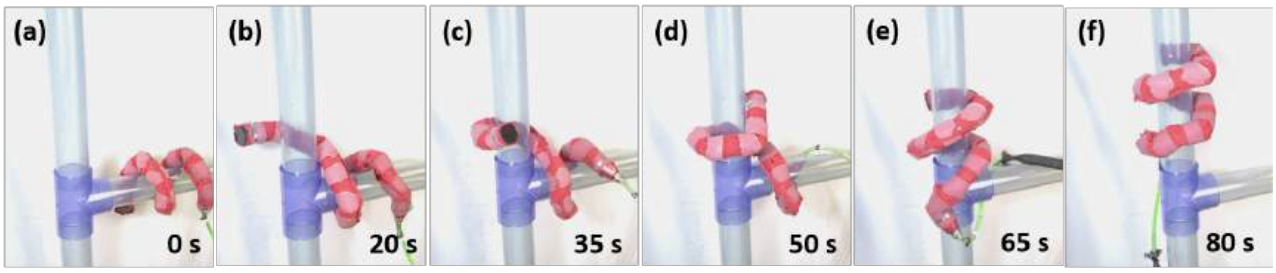

Fig. 10: Stills from videos of the snake robot navigating a T-shaped junction in the vertical plane. The effect of gravity makes this navigation more challenging than a junction in the horizontal plane. Each test involves (a) navigating to the T-shaped junction, (b) bend modules letting go of the source pipe, (c) bend modules wrapping onto the target pipe, (d,e) modules transferring from the source to the target pipe and lastly, (f) navigating away from the T-shaped junction on the target pipe. Of these, all except the first (a) and last (f) steps are performed autonomously.

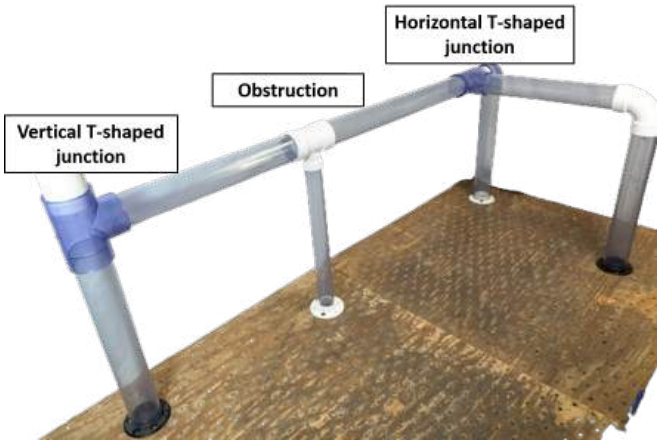

Fig. 11: Pipe network comprised of 3 inch pipes used for testing. This network consists of a horizontal and a vertical T-shaped junction along with a sink pipe treated as an obstruction.

A. User Responsibilities for Gait Execution

During pipe network navigation, the user controls the direction and speed of the robot over straight sections of the pipes. When an obstruction is encountered, the user selects the spiraling gait to navigate around the obstruction. For a brief period, navigation around the obstruction is autonomous, after which control is returned to the user upon successful circumvention.

Similarly, when the snake encounters an intersection, it is the user's responsibility to trigger the windowed rolling helix gait. In particular, the user specifies the module number that is mutually perpendicular to both source and target pipes and lies on the same side of the source pipe as the target pipe (see Fig. 12). Once selected, the transition is performed autonomously, and control is returned to the user after the robot has completely transitioned to the chosen target pipe.

B. Spiraling Gait

Once toggled, the spiraling gait causes the snake robot to execute a screw-like motion to avoid obstacles, as shown in Fig. 8. The linear distance moved by the snake per unit time of spiraling is dependent on the gait parameters as well as the friction between the pipe and snake robot. This constant is pre-characterized and used to determine the length of time to execute spiraling. Parameters used for the spiraling gait are described in Table I.

Parameter	Value
k_r	10
k_p	0.75
m	30
ΔT_s	120s

TABLE I: Spiraling gait parameters used for experiments. The pulse forms a helix with ten times the radius and three quarters the pitch.

C. Windowed Rolling Helix Gait

Depending on the module chosen by the user, the snake infers the polar orientation of the target pipe relative to itself.

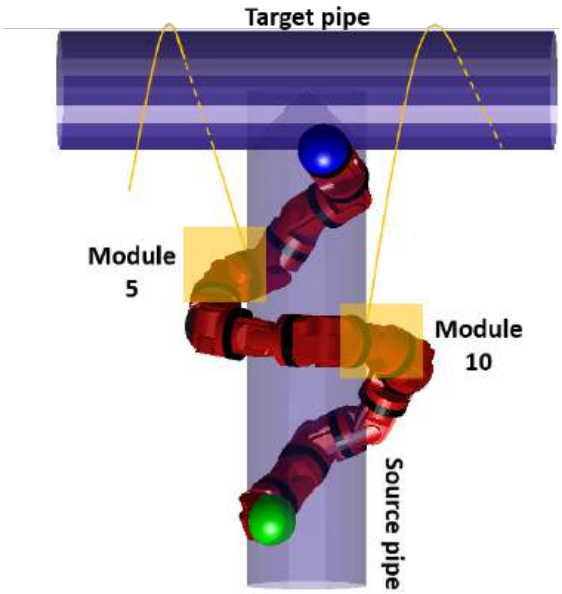

Fig. 12: The user can indicate which side of the pipe to transition to by selecting a module which is mutually perpendicular to both pipes. When the user selects module 5, the snake transitions to the left and when the user selects module 10, the snake transitions to the right.

When this selected module is equal to the optimal number of bend modules calculated in Section V-B.2, the transition can proceed as described in Algorithm 2. When this is not the case, the snake robot executes the spiraling gait to reorient itself around the pipe before attempting the windowed rolling helix gait.

T-shaped junction transitions exhibit varying torque demands due to gravitational forces. A horizontal-to-horizontal transition requires minimal joint torque as it occurs within a gravity-neutral plane. During a vertical-to-horizontal transition, the torque load progressively decreases as the number of modules countering gravity diminishes over time. Conversely, a horizontal-to-vertical transition demands the highest initial torque. This torque load only increases throughout this transition as more modules are recruited to counteract gravity, making it the most demanding scenario. Due to space constraints, we present the horizontal-to-horizontal transition (see Fig. 9) and horizontal-to-vertical transition (see Fig. 10) in this paper.

D. Pipe Diameter Estimation

In these experiments, we assume that the target and source pipes feature the same diameter. To ensure effective wrapping of the bend modules around the target pipe, we estimate the diameter of the source pipe using a virtual chassis technique from Section V-B.4. All tests for the plot (see Fig. 13) were run on a 3 inch pipe with an outer diameter of 88.90 mm (3.5 in). The estimation algorithm is accurate to 10% of the true diameter in 95% of the cases.

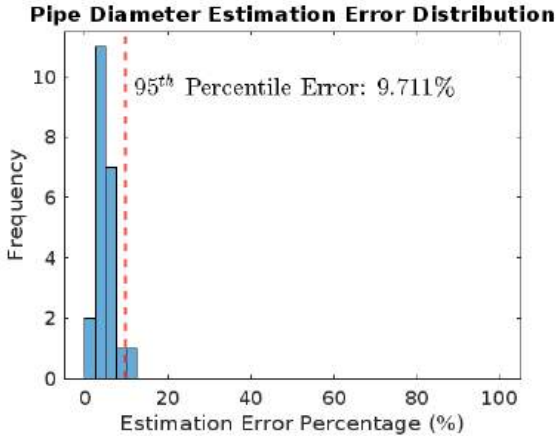

Fig. 13: Error distribution from pipe diameter estimation on 22 tests. The algorithm estimates the diameter of the pipe accurately to within 10% of the true diameter in 95% of cases.

VII. Conclusion

This paper demonstrates the use of snake robots to navigate pipe networks with complex features such as valves or other obstructions and T-shaped junctions. We achieve this with the help of two novel gaits: spiraling and windowed rolling helix. Physical experiments with our SEA snake robot validate the efficacy of these gaits across varying levels of complexity.

Looking ahead, several avenues for future research promise to enhance the capabilities of snake robots in pipe network navigation. A critical advancement would be the elimination of the tether, significantly improving operational autonomy and enabling seamless traversal of sequential pipe network segments.

Furthermore, relaxing the current assumptions of similar pipe diameters and pre-defined robot orientation is crucial. Integrating the compliant motion controller proposed by Travers et al. [25], coupled with the torque-sensing capabilities of our SEA design, offers a promising approach. Additionally, exploring techniques, inspired by [26], to autonomously determine the robot's orientation relative to T-shaped junctions through external torque analysis would further enhance navigational autonomy.

References

[1] Young-Sik Kwon, Bae Lee, In-Cheol Whang, Whee-kuk Kim, and Byung-Ju Yi. A flat pipeline inspection robot with two wheel chains. In *2011 IEEE International Conference on Robotics and Automation*, pages 5141–5146, 2011.

[2] P. Chatzakos, Y. P. Markopoulos, K. Hrissagis, and A. Khalid. On the development of a modular external-pipe crawling omni-directional mobile robot. In *Climbing and Walking Robots*, pages 693–700, Berlin, Heidelberg, 2006. Springer Berlin Heidelberg.

[3] Sang Heon Lee. Design of the out-pipe type pipe climbing robot. *International Journal of Precision Engineering and Manufacturing*, 14:1559–1563, 09 2013.

[4] Jong-Hoon Kim, Gokarna Sharma, and Sheena Iyengar. Famper: A fully autonomous mobile robot for pipeline exploration. In *2010 IEEE International Conference on Industrial Technology*, pages 517 – 523, 04 2010.

[5] Michał Ciszewski, Tomasz Buratowski, and Mariusz Giergiel. Modeling, simulation and control of a pipe inspection mobile robot with an active adaptation system. *IFAC-PapersOnLine*, 51(22):132–137, 2018. 12th IFAC Symposium on Robot Control SYROCO 2018.

[6] G. S. Chirikjian and J. W. Burdick. The kinematics of hyper-redundant robot locomotion. In *IEEE Transactions on Robotics and Automation*, pages 781–793, 1995.

[7] Juan Gonzalez-Gomez, Houxiang Zhang, E. Boemo, and Jianwei Zhang. Locomotion capabilities of a modular robot with eight pitch-yaw-connecting modules. *9th Int. Conf. on Climbing and Walking Robots, Zurich*, 01 2006.

[8] H. Ohno and S. Hirose. Design of slim slime robot and its gait of locomotion. In *Proceedings 2001 IEEE/RSJ International Conference on Intelligent Robots and Systems. Expanding the Societal Role of Robotics in the the Next Millennium (Cat. No.01CH37180)*, volume 2, pages 707–715 vol.2, 2001.

[9] Matthew Tesch, Kevin Lipkin, Isaac Brown, Ross Hatton, Aaron Peck, Justine Rembisz, and Howie Choset. Parameterized and scripted gaits for modular snake robots. *Advanced Robotics*, 23:1131–1158, 06 2009.

[10] Hiroya Yamada and Shigeo Hirose. Steering of pedal wave of a snake-like robot by superposition of curvatures. *2010 IEEE/RSJ International Conference on Intelligent Robots and Systems*, pages 419–424, 2010.

[11] David Rollinson and Howie Choset. Pipe network locomotion with a snake robot. *Journal of Field Robotics*, 33(3):322–336, 2016.

[12] Mariko Inazawa, Tatsuya Takemori, Motoyasu Tanaka, and Fumitoshi Matsuno. Unified approach to the motion design for a snake robot negotiating complicated pipe structures. *Frontiers in Robotics and AI*, 8, 2021.

[13] Tetsushi Kamegawa, Toshimichi Baba, and Akio Gofuku. V-shift control for snake robot moving the inside of a pipe with helical rolling motion. In *2011 IEEE International Symposium on Safety, Security, and Rescue Robotics*, pages 1–6, 2011.

[14] Ross L. Hatton and Howie Choset. Generating gaits for snake robots by annealed chain fitting and keyframe wave extraction. In *2009 IEEE/RSJ International Conference on Intelligent Robots and Systems*, pages 840–845, 2009.

[15] Weikun Zhen, Chaohui Gong, and Howie Choset. Modeling rolling gaits of a snake robot. *Proceedings - IEEE International Conference on Robotics and Automation*, 2015:3741–3746, 06 2015.

[16] G S Chirikjian and J W Burdick. A modal approach to hyper-redundant manipulator kinematics. *IEEE Transactions on Robotics and Automation (Institute of Electrical and Electronics Engineers)*, 10:3, 06 1994.

[17] Shigeo Hirose. *Biologically Inspired Robots (Snake-like Locomotor and Manipulator)*. Oxford University Press, 1993.

[18] Hiroya Yamada and Shigeo Hirose. Study on the 3d shape of active cord mechanism. *Proceedings 2006 IEEE International Conference on Robotics and Automation, 2006. ICRA 2006.*, pages 2890–2895, 2006.

[19] Mizuki Nakajima, Qi Cheng, and Motoyasu Tanaka. Gait design and experimental validation of a snake robot on a pipe with branches using spiral stairs function. *Artificial Life and Robotics*, 27, 03 2022.

[20] Wei Qi, Tetsushi Kamegawa, and Akio Gofuku. Proposal of helical wave propagate motion for a snake robot to across a branch on a pipe. In *2016 IEEE/SICE International Symposium on System Integration (SII)*, pages 821–826, 2016.

[21] J. Dai et al. Robot-inspired biology: The compound-wave control template. In *IEEE International Conference on Robotics and Automation (ICRA)*, pages 5879–5884, Seattle, WA, USA, 2015.

[22] F. Ruscelli. Shape-based compliance control for snake robots. Master's thesis, University of Bologna, 2016.

[23] David Rollinson and Howie Choset. Virtual chassis for snake robots. In *2011 IEEE/RSJ International Conference on Intelligent Robots and Systems*, pages 221–226, 2011.

[24] David Rollinson, Yigit Bilgen, Ben Brown, Florian Enner, Steven Ford, Curtis Layton, Justine Rembisz, Mike Schwerin, Andrew Willig, Pras Velagapudi, and Howie Choset. Design and architecture of a series elastic snake robot. In *2014 IEEE/RSJ International Conference on Intelligent Robots and Systems*, pages 4630–4636, 2014.

[25] M. Travers, J. Whitman, and H. Choset. Shape-based compliance in locomotion. In *Proceedings of Robotics: Science and Systems (RSS '16)*, pages 20 – 28, June 2016.

[26] S. Pellegrini. Snake robot gaits and proprioceptive methods for pipe network navigation. Master's thesis, Ecole Polytechnique Federale de Lausanne, 2024.